$\mathcal{H}_\infty$ loop shaping design for nano-positioning

Abu Sebastian[1†], Srinivasa Salapaka[2‡]

[1]abuseb@iastate.edu, [2]svasu@mit.edu

[†]Department of Electrical and Computer Engineering, Iowa State University, Ames, IA 50011

[‡] Laboratory of Information and Decision Systems, Massachusetts Institute of Technology, MA 02139

Abstract

This article presents the identification and control of a nano-positioning device. The device consists of two stages which enable two dimensional positioning. Each stage is actuated by piezo-electric stacks and its motion is sensed by a Linear Variable Differential Transformer (LVDT). A 2×2 transfer function has been identified to describe the device. In this paper the main limitations to nano-positioning have been overcome through control. Feedback laws have been designed to address the undesirable effects of hysteresis and creep which are significant in the open loop implementation and to meet the steady state tracking and bandwidth requirements of nano-positioning. Great emphasis has been placed on robustness which leads to a system that can withstand the diverse conditions where it will be used and does not necessitate tuning as is the case with the existing designs. Accordingly, Glover-McFarlane $\mathcal{H}_\infty$ loop shaping controllers have been employed to robustify existing non-model based designs. The merits of these designs along with the experimental results obtained by using them have been presented.

Introduction

The last two decades have seen the rise and the growth of nanoscience and nanotechnology. The growth of research in these areas and the rapid rise in their applications, has in turn imposed new demands on nanotechnology. One of the most central demands are devices capable of high precision positioning. Besides this requirement, many applications require fast positioning systems. This necessitates the design of high precision and high bandwidth nano-positioning devices.

Typically, the nano-positioning devices are actuated by piezoelectric materials. However, their use is hindered by nonlinear effects like hysteresis and creep. There have been many efforts to counter the nonlinear effects which include design changes in the open-loop implementation such as: using 'harder' piezoceramics which have smaller nonlinear effects at the cost of travel range; replacing voltage control by charge control (see Ref. [1]) which achieves lower hysteresis but leads to more creep, lesser travel and lower positioning bandwidth; post processing data obtained from actuations designed for pre-specified trajectories (see Ref. [2]), which are not useful for applications that need real time compensations; and compensating for the adverse nonlinear effects by a careful modeling of the nonlinearities which achieves good results but is very sensitive to the models obtained. In comparison with open loop architecture there are fewer feedback design schemes for nano-positioning. In Ref. [3], the design of a feedback controller using an optical sensor attachment to enhance the performance of an Atomic Force Microscope scanner (cylindrical) has been described. Similar efforts to improve the scanning speeds of the AFM are made in Ref. [4]. Ref. [5] describes the $\mathcal{H}_\infty$ controller design for a one dimensional nano-positioning system (independent of the AFM). There, it was also shown that Proportional-Integral feedback laws, which are typically used in the nano-positioning industry, are incapable of achieving high bandwidth for these systems.

In this article, a nano-positioning system capable of positioning in two dimensions is presented. This device has a complex design and the transfer functions that model the dynamics of motion vary with time and operating regime. Hence there is a need for a robust control approach to control design. The Glover McFarlane loop shaping design is used to robustify the non-model based designs which lack robustness. Experimental results show the usefulness of this approach. In Section 1 a description of the device is given. This is followed by frequency domain based system identification described in Section 2. The control design and the experimental results are presented in Section 3. Further results on tackling nonlinear effects using feedback and a characterization of the system in terms of resolution, sensitivity etc. is presented in Section 4.

1 Device description

The nano-positioning system was developed by *Asylum Research*, Santa Barbara, California. It consists of a flexure system, an actuation system, a detection system and a control system. The flexure stage consists of two stages, 'X' seated on 'Y' (see Figure 1), with the sample holder on the 'X' stage. Each stage by virtue of the serpentine spring design deforms under the application of force and thus provides motion.

0-7803-7896-2/03/$17.00 ©2003 IEEE

Proceedings of the American Control Conference
Denver, Colorado June 4-6, 2003

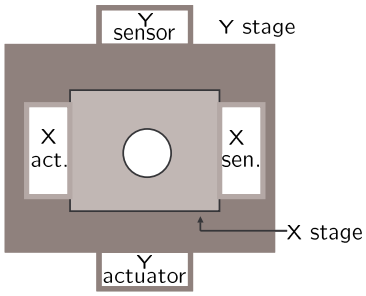

Figure 1: A schematic of the nano-positioning device. There are two stages 'X' and 'Y' with 'X' sitting on top of 'Y'. Each stage is actuated by piezo-electric stacks and the resulting motion is sensed by LVDT sensors.

The forces are applied to the stages at orthogonal directions. These forces are generated by stack-piezos and the high voltage inputs are provided by voltage amplifiers. We will refer to the amplifier-piezo combination as the actuation system. The motion of each stage is sensed and measured by the respective LVDT and the associated demodulation circuit. These actuators lead to a travel range of approximately $100\mu m$ in both directions. The modified LVDT sensors (developed by *Asylum Research*) used in this design have resolution in the order of $2\mathring{A}$ over $1KHz$ bandwidth. In this device, the control laws were implemented using an *Analog Devices ADSP-21160* digital signal processor.

2 Identification

The complex structural design makes physical modeling of the device difficult. The model has been inferred using frequency response based techniques. The device is viewed as a two-input two-output system where the low voltage signals to the 'X' and 'Y' amplifiers (u_x and u_y) are the inputs and the motion of 'X' and 'Y' stages measured by the respective LVDT sensors, (x and y) are the outputs. This results in four input-output transfer functions, $G_{ji}, j, i \in \{x, y\}$. Here G_{ji} represents the transfer function from the input u_i to the output j. Figure 2 depicts the different blocks constituting the mapping between u_x and x. These maps

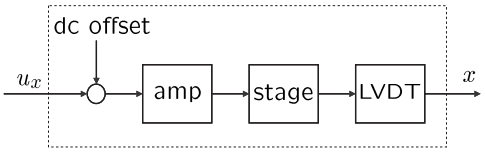

Figure 2: u_x is the input to the amplifier which drives the stack piezo. The motion of the stage is sensed using an LVDT sensor whose output is x.

can be assumed to be linear over a small region of operation about an operating point. The nominal operating point was chosen to be the 'null position', i.e. where the LVDT outputs read zero. Frequency responses were obtained about this operating point to obtain the nominal model denoted by,

$$G = \begin{bmatrix} G_{xx} & G_{xy} \\ G_{yx} & G_{yy} \end{bmatrix}$$

The responses were obtained using a *HP3536A* signal analyzer with $10mV$ amplitude forcing and averaged over 200 measurements. The responses were obtained over a bandwidth of $1.25kHz$. Rational transfer functions were fit to the responses. $G_{xx}(s)$ is a 7th order transfer function with the first resonance frequency at $\approx 390Hz$. $G_{yy}(s)$ is 5th order with the first resonance frequency at $\approx 235Hz$. Figure 3 show how well the frequency response obtained from the model agrees with that obtained experimentally.

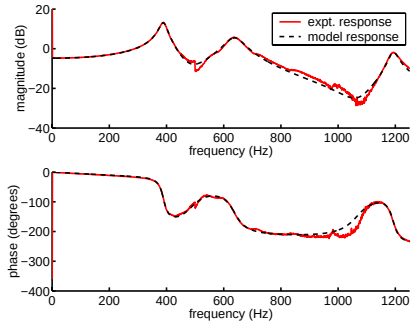

Figure 3: Experimental frequency response is compared with the response of the model $G_{xx}(s)$.

In order to further verify the models, step responses obtained experimentally were compared with the model responses. To study the variation of these models to the operating points, frequency responses were obtained at different operating points. A considerable variation was observed in these responses. Figure 4 shows the responses obtained at different operating points over a range of $\approx 80\mu m$ separated by $\approx 20\mu m$. Further it was observed that the frequency response at the same operating point varies when obtained at different times. These uncertainties in the model make robustness of the closed loop system a key requirement. The design of the feedback laws to achieve these requirements is presented in the next section.

3 Controller design and implementation

Open loop operation of the device is not satisfactory for a number of reasons. The model of the device is uncertain which makes it difficult to prescribe appropriate reference signals. The hysteresis and creep effects are dominant and limit the use of the device (these effects have been presented in Section 4). The main design

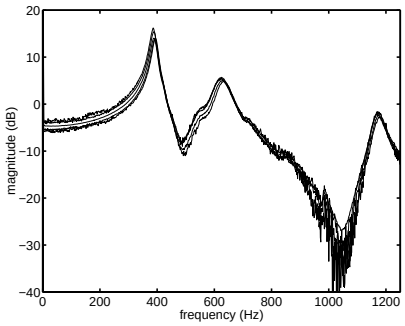

Figure 4: Experimentally obtained frequency responses at different operating regions for the X stage.

goals of control design are of achieving high precision tracking with high bandwidths, compensating the adverse effects of hysteresis and creep and achieving robustness of the closed loop map towards model uncertainties.

In the design of the feedback laws, the coupling transfer functions G_{xy} and G_{yx} are neglected in order to obtain lower order control laws. This is reasonable as the coupling terms are relatively small. The mode of operation of this device is such that higher bandwidth requirements are made on the smaller stage 'X' where as 'Y' stage is made to move relatively slow. Hence, there is a greater emphasis on the control designs for the 'X' stage which is presented in this paper. Designs were also done for G_{yy} and the resulting diagonal controllers were implemented, the details of which are not addressed in this paper. Figure 5 shows a SISO feedback loop for the 'X' stage. In this figure, x_r is the reference signal, the

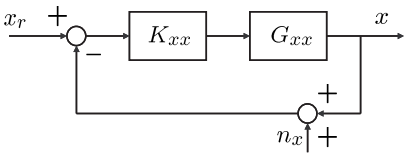

Figure 5: A unity feedback configuration for G_{xx}.

output signal is x and K_{xx} is the control transfer function that needs to be designed. The error e_x is given by, $e_x = x - x_r = -Sx_r - Tn_x$, where the sensitivity function, $S = 1/(1 + G_{xx}K_{xx})$ and the complementary sensitivity function $T = G_{xx}K_{xx}/(1 + G_{xx}K_{xx})$. The frequency at which $|S(j\omega)|$ crosses -3dB is defined as the closed loop bandwidth. $\|T\|_\infty$ and $\|S\|_\infty$ are measures of the robustness of the closed loop system. The design, analysis and implementation of control laws are presented in this section.

3.1 Control designs

3.1.1 Non model based controllers:

Proportional double integral (PII) control design: Proportional integral (PI) and proportional double integral (PII) controllers are the most common forms of controllers currently used for nano-positioning in the scanning-probe industry. Their popularity stems from the fact that they track ramp signals (common in imaging applications) with zero steady state errors. Here, two PII designs are presented which have been obtained after considerable search and tuning over the parameter space. They are given by $K_{pii1}(s) = \frac{0.001s^2+450s+10^5}{s^2}$ and $K_{pii2}(s) = \frac{0.001s^2+450s+2\times10^5}{s^2}$. The second controller is designed for a larger bandwidth ($38 > 32$) at the cost of robustness. The simulated complementary sensitivity function $T(j\omega)$ for each closed loop system is shown in Figure 6. It is seen that for both these designs, the bandwidths are low and have poor robustness properties which is evident from the large spikes in the $T(j\omega)$ plots. Figure

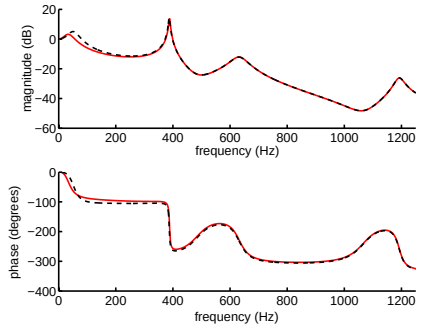

Figure 6: $T(j\omega)$ for PII designs. The large values of $\|T\|_\infty$ is indicative of the low robustness of these designs.

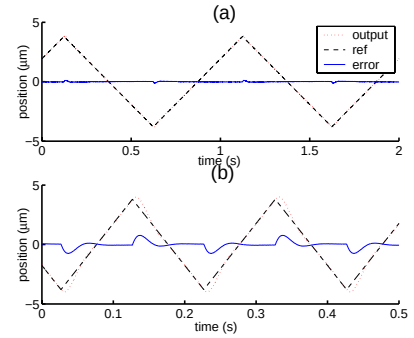

Figure 7: This figure shows the tracking of triangular reference signals using a PII controller. At $5Hz$, oscillatory behavior is observed.

7 shows the tracking of $1Hz$ and $5Hz$ triangular waves using K_{pii1}. The tracking errors at turn around points are large since these contain higher harmonics which the device does not track. However, this does not pose a significant problem as the data corresponding to this region is discarded in a typical scanning application. But it is important that in the mid regions, the trian-

gular wave is tracked satisfactorily. The $5Hz$ tracking is quite unsatisfactory as there is substantial error over the whole trajectory. Experiments show that the robustness is very low. Attempts to introduce a filter within the loop to improve the resolution often results in instability. This is expected as the phase margins are very small.

3.1.2 Glover-McFarlane control design: Here, we present an elegant control design introduced by Glover and McFarlane (Ref. [7] and Ref. [8]). This design process consists of two steps:

1. shaping of the loop transfer function: In this step, a shaping transfer function K_s is designed to shape the plant in order to have certain closed loop characteristics. In this design, K_s is set equal to a PII controller. This was done to retain the closed loop property of tracking ramp signals with zero steady state error.

2. design of a robustifying controller: In this step, a robustifying controller K_r is obtained which gives good robustness properties to the closed loop system obtained from the shaped plant $G_s = K_s G_{xx}$ of the previous step.

More specifically, in the second step, a controller is sought to stabilize a class of plants described by,

$$\{(M+\Delta_M)^{-1}(N+\Delta_N) : \| \begin{bmatrix} \Delta_N & \Delta_M \end{bmatrix} \| \leq \epsilon\}$$

where $G_s = \frac{N}{M}$ is the normalized left coprime factorization of the the nominal shaped plant. ϵ which is called the stability margin is a measure of the robustness of the design. It can be shown that the maximum possible ϵ is given by $\epsilon_{max} = \{1 - \| \begin{bmatrix} N & M \end{bmatrix} \|_H^2\}^{1/2}$ where $\|.\|_H$ denotes the Hankel norm (see Ref. [7]). Usually an $\epsilon < \epsilon_{max}$ is used for the design of the robustifying controller which is *explicitly* given in terms of the positive definite solutions of two Algebraic Riccati Equations which depend only on the parameters of the shaped plant (see [6] for details).

The coprime uncertainty characterization seems to be appropriate for nano-positioning devices which typically exhibit low frequency parametric uncertainty and high frequency unmodeled dynamics. Multiplicative uncertainty characterization is more suitable for unmodeled dynamics where as inverse multiplicative uncertainty characterization is more appropriate for parametric uncertainty. The coprime uncertainty characterization is an elegant mixture of both, with uncertainty in M resembling inverse multiplicative uncertainty and that in N resembling multiplicative uncertainty. From the norm bound, $\| \begin{bmatrix} \Delta_N & \Delta_M \end{bmatrix} \| \leq \epsilon$ it follows that,

$$\epsilon^2 \geq \frac{|\hat{\Delta M}(j\omega)|}{1+|G_s(j\omega)|^2} + \frac{|\hat{\Delta N}(j\omega)|}{1+\frac{1}{|G_s(j\omega)|^2}},$$

where $\hat{\Delta M} = \frac{\Delta M}{M}$ and $\hat{\Delta N} = \frac{\Delta N}{N}$. This implies that at frequencies where the shaped plant $|G_s(j\omega)|$ is large, more parametric uncertainty is permitted where as where $|G_s(j\omega)|$ is small, more unmodeled dynamics is allowed (see Ref. [9]). The PII control laws shape the loop transfer function G_{xx} in such a way that G_s is large at low frequencies where parametric uncertainty due to the nonlinear effects is more dominant and G_s is small at high frequencies where unmodeled dynamics is the primary cause of uncertainty. Another important feature of the Glover McFarlane design is that the loop transfer function before and after robustification is not significantly different (Ref. [8]).

This design process was applied to G_{xx} with many shaping functions, K_s. First K_s was set to be K_{pii1}. A 9th order robustifying controller K_r was obtained.

Figure 8 compares the experimentally obtained $S(j\omega)$ for K_{pii1} before and after robustification. There is substantial reduction in the peak of $|S(j\omega)|$ due to the robustifying controller. The guaranteed gain and phase margins given in terms of $\|S\|_\infty$ are GM $= \|S\|_\infty/(1-\|S\|_\infty)$ and PM $= 2\sin^{-1}(1/2\|S\|_\infty)$. The resulting GM and PM for the Glover McFarlane design is 2.3 and 33 degrees respectively which are significantly higher than 1.2 and 12.8 degrees for K_{pii1}. Note that the bandwidth is comparable for both in spite of the significant difference in robustness. Much more aggressive PII controllers were implemented with the help of robustification. This include controllers which made the closed loop unstable when used without robustification. Experimental $S(j\omega)$ for various Glover McFarlane designs are presented in Figure 9. These plots show significant increase in bandwidth ($> 55Hz$) without much loss in robustness. Figure 10 illustrates the tracking of $5Hz$ and $10Hz$ signals using a Glover McFarlane design. There is a significant region over the trajectory where the error is small. Also these controllers are remarkably robust allowing the use of filters inside the loop to improve resolution.

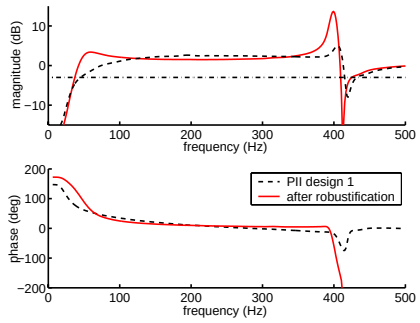

Figure 8: Experimentally obtained $S(j\omega)$ of K_{pii1} before and after robustification.

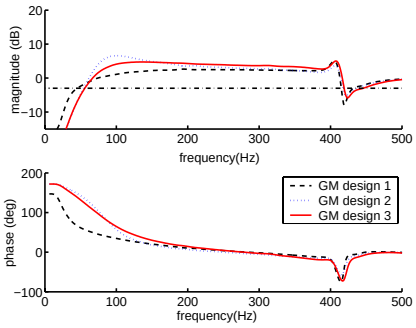

Figure 9: Sensitivity plots of the Glover McFarlane designs

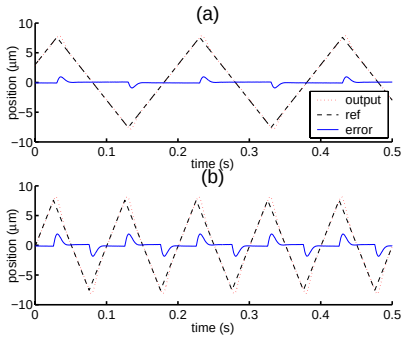

Figure 10: Tracking of $5Hz$ and $10Hz$ triangular signals using a Glover McFarlane controller. Except for the turn around regions, the tracking is very good.

3.2 Control design implementation

The controllers designed in section 3.1 were discretized and implemented on an Analog Devices ADSP-21160 Digital Signal Processor. The analog signals were sampled at 100kHz. The discretized controllers were split into biquad sections (second order sections) and each biquad was implemented in a Direct Form II IIR structure. This cascade implementation allows optimum pole-zero pairing and ordering which can be used to counter finite word length effects (see Ref. [10]).

4 Characterization of the device

In this section the device is characterized in terms of static sensitivity, range, resolution, in the open and closed loop configurations. The Glover McFarlane closed loop design is presented as an example to study how nonlinear effects are addressed by feedback.

4.1 Static sensitivity and travel range

The device was calibrated using a grating. The sensitivity of the LVDT was found to be $6.76\mu m/V$. The total travel range of each stage is $\approx 100\mu m$.

4.2 Resolution

Since the transfer function between x and n is T, $(x = Tx_r - Tn)$ this transfer function forms a good basis to characterize and compare different designs in terms of resolution. This transfer function brings forth the trade off that exists between the resolution and the bandwidth. This is seen from the fact that higher bandwidth implies bigger error signals and therefore larger resolutions. The resolutions can be characterized by associating appropriate metrics to the error signals $e_x = Tn$ if enough statistics describing n is available. This presents us with one of the problems we have with the characterization of resolution. It is the fact that our measurements are limited by the resolution of the LVDT sensors, i.e., the device is capable of motions that are smaller than that which LVDT can detect. However, to get a quantitative feel of how small these error signals can be, the following experiment was done. The LVDT signals for both the open-loop and the closed-loop (Glover McFarlane) designs were measured when the system is at the nominal operating point. the measurement is taken over a small time window since in open loop the mean varies with drift, creep etc. Figure 11 shows that the variance of the sensor output while in open loop is higher than that in closed loop. This illustrates the improvement in 'resolution' due to feedback. It should be remembered that the closed loop resolution depends on the bandwidth and the shape of the corresponding complementary sensitivity functions. Better resolutions can be achieved by reducing the bandwidths.

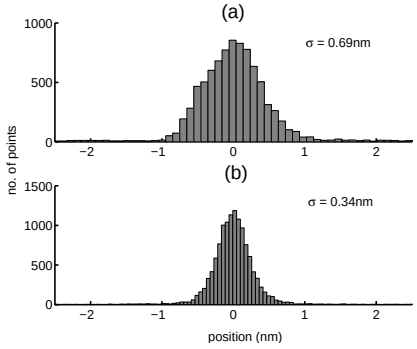

Figure 11: a) LVDT measurement without the controller. b) LVDT measurement while a controller is stabilizing at 0V.

4.3 Elimination of nonlinear effects

As mentioned earlier, the application of the piezoactuated devices are greatly limited by nonlinear effects such as hysteresis and creep. However these effects are nearly eliminated by the feedback designs described earlier. Hysteresis is primarily due to the nonlinear relationship between the input voltages and the piezo displacements. Its effects are big when the scan travels are large. To present the efficacy of the feedback designs, the hysteresis curves obtained in open-loop are com-

pared with the closed-loop device obtained by Glover-McFarlane design. The hysteretic effects become more dominant as the scan size is increased. In a travel of $40\mu m$, a maximum output hysteresis of $\approx 3\mu m$ (7.5%) was observed. The same experiment with the closed-loop device showed that these effects were practically eliminated (see Figure 12). It should be noted that input signals as big as $5V$ were given while the nominal system was identified using just $10mV$ signals and still the input-output relation is linear. This emphasizes the greatly increased linearity of the device. Creep is another undesirable nonlinear effect that was addressed by our feedback design.

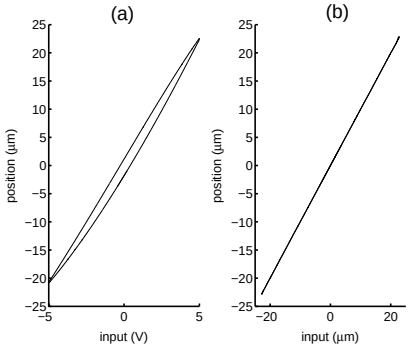

Figure 12: (a) Hysteretic behavior while moving the X stage in open loop. (b) A Glover McFarlane controller is used to remove hysteresis.

5 Conclusions

The identification and control of a two dimensional nano-positioning stage is presented. The non-model based controllers are compared with advanced controllers like Glover McFarlane and $\mathcal{H}_\infty$ controllers. These designs result in significant improvement in robustness in addition to gain in bandwidth and resolution. This paper illustrates the significance of a robust control approach in the field of nano-positioning. The requirements of nano-positioning fall naturally into the robust control framework. Further research in this area could be the design of MIMO controllers where the cross-coupling between the 'X' and 'Y' stages is addressed.

Acknowledgements

This research is supported by NSF grants ECS-9733802 and CMS-0201560 and the DARPA-MOSAIC program. We would like to acknowledge the constant support of Prof. Murti Salapaka of Iowa State University and Dr. Jason Cleveland of *Asylum Research*. Thanks are also due to Todd Day, Dan Bocek, Dr. Mario Viani and others in *Asylum Research* for all the help during the course of the project.

References

[1] H. Kaizuka. Application of capacitor insertion method to scanning tunneling microscopes. *Rev. of Sci. Instrum.*, 60(10):3119–3122, 1989.

[2] R.C. Barrett and C.F. Quate. Optical scan-correction system applied to atomic force microscopy. *Rev. of Sci. Instrum.*, 62:1393–1399, 1991.

[3] A. Daniele, S. Salapaka, M.V. Salapaka, and M. Dahleh. Piezoelectric Scanners for Atomic Force Microscopes:Design of Lateral Sensors, Identification and Control. In *Proceedings of the American Control Conference, San Diego, California*, pages 253–257, June 1999.

[4] G. Schitter, P. Menold, H. F. Knapp, F. Allgower, and A. Stemmer. High performance feedback for fast scanning atomic force microscopes. *Review of Scientific Instruments*, 72(8):3320–3327, August 2001.

[5] S. Salapaka, A. Sebastian, J. P. Cleveland, and M. V. Salapaka. High bandwidth nano-positioner: A robust control approach. *Review of Scientific Instruments*, 73(9):3232–3241, September 2002.

[6] S. Skogestad and I. Postlethwaite. *Multivariable Feedback Control, Analysis and Design*. John Wiley and Sons, 1997.

[7] K. Glover and D. McFarlane. Robust stabilization of normalized coprime factor plant descriptions with $\mathcal{H}_\infty$-bounded uncertainty. *IEEE transactions on automatic control*, 34(8):821–830, August 1989.

[8] D. McFarlane and K. Glover. A loop shaping design procedure using $\mathcal{H}_\infty$ synthesis. *IEEE transactions on automatic control*, 37(6):759–769, June 1992.

[9] G. Vinnicombe. *Uncertainty and Feedback: $\mathcal{H}_\infty$ loop-shaping and the ν-gap metric*. Imperial College Press, 2001.

[10] S. K. Mitra. *Digital Signal Processing: A computer based approach*. McGraw-Hill, 2nd edition edition, 1999.